

Star Formation in Disks: Spiral Arms, Turbulence, and Triggering Mechanisms

Bruce G. Elmegreen¹

¹IBM Research Division, T.J. Watson Research Center, 1101 Kitchawan Road,
Yorktown Hts. 10598, USA
email: bge@us.ibm.com

Abstract. Star formation is enhanced in spiral arms because of a combination of orbit crowding, cloud collisions, and gravitational instabilities. The characteristic mass for the instability is $10^7 M_{\odot}$ in gas and $10^5 M_{\odot}$ in stars, and the morphology is the familiar beads on a string with 1-2 kpc separation. Similar instabilities occur in resonance rings and tidal tails. Sequential triggering from stellar pressure occurs in two ways. For short times and near distances, it occurs in the bright rims and dense knots that lag behind during cloud dispersal. For long times, it occurs in swept-up shells and along the periphery of cleared regions. The first case should be common but difficult to disentangle from independent star formation in the same cloud. The second case has a causality condition and a collapse condition and is often easy to recognize. Turbulent triggering produces a hierarchy of dense cloudy structure and an associated hierarchy of young star positions. There should also be a correlation between the duration of star formation and the size of the region that is analogous to the size-linewidth relation in the gas. The cosmological context is provided by observations of star formation in high redshift galaxies. Sequential and turbulent triggering is not yet observable, but gravitational instabilities are, and they show a scale up from local instabilities by a factor of ~ 3 in size and ~ 100 in mass. This is most easily explained as the result of an increase in the ISM turbulent speed by a factor of ~ 5 . In the clumpiest galaxies at high redshift, the clumps are so large that they should interact with each other and merge in the center, where they form or contribute to the bulge.

Keywords. stars: formation, ISM: evolution, galaxies: formation, galaxies: high-redshift

1. Star Formation in Spiral Arms

Star formation in local disk galaxies, including the Milky Way, is highly concentrated in spiral arms. This is partly because the gas is concentrated in the arms as a result of density-wave streaming. The stellar spiral arm potential pulls out the interarm gas nearly radially, causing it to traverse the interarm region quickly, and it shocks and pulls back the gas when it enters the arm, causing it to deflect and move nearly parallel to the arm. Because the time spent at each position relative to an arm is inversely proportional to the perpendicular component of the velocity, and because the local density is also inversely proportional to this velocity, the gas lingers in an arm for a time proportional to its density. Thus most star formation occurs where the arm is dense because most of the time and most of the gas occurs there. If this were all that happened, then the star formation rate should be directly proportional to the total gas density in an azimuthal profile around the disk. There are no recent studies of the azimuthal dependence of star formation, although more on this topic was done over a decade ago (e.g., Garcia-Burillo *et al.* 1993). In addition to this purely kinematical effect, there may also be a dynamical effect in the sense that the star formation rate per unit gas mass increases in the arms relative to the interarm regions. In this case, the star formation rate should increase with the total gas density to a power greater than unity for azimuthal profiles. In either case,

the sizes of the star-forming regions are much larger in the arms than between the arms (e.g., Lundgren *et al.* 2004).

Consideration of dynamical processes and the time available suggest that spiral arms could promote local gravitational instabilities that trigger star formation in giant complexes (e.g., Tosaki *et al.* 2002). In the low-shear environment of an arm (e.g., Luna *et al.* 2006), such instabilities produce $10^7 M_{\odot}$ clumps rather than spiral wavelets. Magnetic fields help by removing gas angular momentum during subsequent collapse (Kim & Ostriker 2002). The morphology of star formation then consists of HI clouds with molecular cores lining the stellar spiral arms (e.g., Engargiola *et al.* 2004). Feathers and spurs extend into the interarm region as the arm clouds feel an increased shear (e.g., La Vigne *et al.* 2006). Deep in the interarm regions, star formation lingers in the long-lived envelopes and diffuse debris of spiral arm clouds (Elmegreen 2007).

In galaxies without strong stellar spirals, star formation occurs throughout the disk in flocculent arms that are probably the result of local, swing-amplified instabilities (e.g., Fuchs *et al.* 2005). Thus, star-forming clouds form or grow in (1) spiral-wave triggered gravitational instabilities and cloud collisions in dense dust lanes, and (2) random gravitational instabilities everywhere if there are no stellar spirals, or if the stellar spirals are weak. In either case, star formation follows cloud formation in a few cloud dynamical times. It lingers and gets triggered at a low level in the molecular cloud debris for a much longer time.

2. Triggering

Triggering of star formation is well known in places like the pillars of M16 (Hester *et al.* 1996), and other bright rims (e.g., Sugitani *et al.* 1989; Reach *et al.* 2004). The large-scale structure of Ophiuchus also suggests that the main star formation was triggered in the head of a cometary cloud shaped by pressures from the Sco-Cen OB association (de Geus 1992). Other triggering takes the form of shells, with old stars in the center and young stars along the periphery. Such shells have been observed in local star-forming regions (e.g., Zavagno *et al.* 2006) and in other galaxies (e.g., Brinks & Bajaja 1986). Some triggering shells can be very large (Wilcots & Miller 1998; Walter & Brinks 1999; Yamaguchi *et al.* 2001a) and some contain triggered pillars also (e.g., Yamaguchi *et al.* 2001b; Oey *et al.* 2005).

Generally, the spatial scale for triggering is the shock speed in the ambient gas multiplied by the timescale for the pressure source, $L \sim (P/\rho_0)^{1/2} \times T$. If the spatial scale is smaller than the cloud in which the first generation of star formation occurs, then pillars and bright rims form by the push-back of interclump gas. Star formation triggering can be fast in this case, prompted by the direct squeezing of pre-existing dense gas. Also in this case, the relative velocity of the triggered stars will be small because they are in the dense gas that is left behind. If the triggering scale is larger than the size of the cloud, then shells form by the push-back of all the gas, both in the cloud and in the intercloud medium. This is a slow process because new clumps have to form, and the time scale for this is $\sim (G\rho_{shell})^{-1/2}$. The velocity of triggered stars in this second case can be large, comparable to the shock speed, $\sim (P/\rho_0)^{1/2}$. There is also a causality condition, where the triggering distance between generations equals the time difference multiplied by the velocity difference. Criteria for gravitational collapse in expanding shells were derived by Elmegreen (1994), Elmegreen, Palous & Ehlerova (2002), and Whitworth *et al.* (1994).

There are many types and sources of energy in the ISM and many possible causes for triggering. Energy *types* include thermal, magnetic, turbulent, cosmic ray, and rotational. The first four are all comparable and equal to several tenths of an eV cm^{-3} . Rotational energy is much denser, several hundred eV cm^{-3} . Of the first four, only supersonic turbulence has been associated with star formation triggering because such turbulence can compress the gas a lot. Thermal instabilities compress the gas too, but usually in small regions where self-gravity is not important. Magnetic fields cause slight compression when the gas rearranges itself on the field lines following a Parker instability, but this rearrangement alone is not enough to trigger star formation – that requires self-gravity too. Cosmic rays interact with the ISM primarily through heating and the generation of small scale MHD turbulence. If this turbulence compresses the gas significantly, and on sufficiently large scales, then cosmic rays could trigger star formation (there has been no theoretical work on this mechanism as far as I know). Rotational energy compresses the gas and triggers star formation more than any of the others when something gets in the way of the uniform circular motion. Then a galactic-scale shock forms and star formation results in the dense gas. Spiral density waves in the stars and stellar bars can do this, as mentioned in the previous section.

Among the various *sources* of ISM energy, we include supernovae, HII regions and stellar winds as stellar sources, and galaxy rotation as an energy source for the magnetic field through the dynamo. The magnetic field drives turbulence and convection into the halo by the Parker instability (e.g., Kosiński, & Hanasz 2006; Lee & Hong 2007), and it drives turbulence in the midplane by amplifying epicyclic oscillations in the radial direction, which is the Magneto-Rotational instability (e.g., Kim, Ostriker, & Stone 2003). Galactic rotation also generates turbulence at spiral waves (Bonnell, *et al.* 2006; Kim, Kim, & Ostriker 2006; Dobbs & Bonnell 2007). In addition, there is star-light energy, which is comparable in density to turbulence, cosmic rays, and other energies mentioned above, but is not so easily coupled to the gas. There is also ISM self-gravity, which may be considered as a source of energy for motions if it is replenished by cloud disruption, in which case the real energy source is that of the disruption (i.e., young stars; self-gravity only stores the other energies in potential form.)

Of these sources, most do not trigger star formation because they do not interact with gas in the right way. The most important energy sources are those that produce high pressures for long times – long enough for gravity to act in the compressed regions. Single supernovae, for example, are short-lived, with radiative lifetimes only a percent of the local dynamical time of the gas they are in (Dekel & Silk 1986). Magnetic energy, cosmic rays, and starlight do not compress the gas much. HII regions and O-star winds compress only the most local gas, but they do this for a long time and often trigger star formation in adjacent molecular clouds. Combined pressures from HII regions, winds and supernovae can cause major triggering: they act in OB associations for a relatively long time, ~ 5 Myr or more, and can trigger star formation on a scale of 10 to 100 pc or more in the surrounding gas, which includes remnants of the molecular clouds that formed these stars, neighboring molecular clouds, and intercloud gas.

In summary, star formation either follows cloud formation, or it is stimulated in existing clouds by external processes. Gaseous self-gravity alone triggers cloud formation through: (1) dust-lane fragmentation in stellar density waves, (2) ring fragmentation in Lindblad resonance rings, (3) tidal clump or dwarf galaxy formation in the tidal arms of interacting galaxies, and (4) swing amplified clumps if there are no imposed stellar structures. Self-gravity also causes existing clouds to collapse and fragment into denser pieces where stars form. The morphologies of these processes are relatively easy to recognize in ideal

cases: they appear as “beads on a string” of star formation in spiral arms, resonance rings, and tidal tails, or they are sheared spiral-like clumps from local instabilities in the gas. All of the clouds or cores formed by self-gravity have masses exceeding the relevant Jeans mass. In the case of instabilities in disks, filaments and shocked layers, the elongated regions are always unstable to condensation into spheroids. If the resulting spheroids are massive enough, then they can collapse further into clusters or single stars. If the disk is rotating, or the layer is expanding, then the largest scales are stabilized and there is a column density threshold that has to be exceeded so that regions large enough to exceed the Jeans length (where gravity exceeds pressure) are also smaller than the stabilization length (where rotation or expansion exceed gravity).

Inside the clouds formed by these processes, star formation is also triggered by locally high pressures from HII regions, winds, and multiple SNe, and from cloud collisions, or in supersonically turbulent media, by compressions from converging flows. All of these compressions tend to enhance magnetic diffusion and decrease the dynamical time. The morphology of this triggering is also fairly easy to recognize in ideal cases because the compressed regions are shells, comets, and moving layers, all adjacent to high pressures, and all with the causality constraint mentioned above.

3. Turbulence Triggering

The compressed regions in a supersonically turbulent cloud act like seeds for gravitational attraction and can lead to the local accretions necessary to make stars (see reviews in Mac Low & Klessen 2004; Bonnell *et al.* 2007). Simulations by several groups have shown how turbulence in a cloud core can produce a star cluster (e.g., Li *et al.* 2004; Bate & Bonnell 2005; Jappsen *et al.* 2005; Padoan *et al.* 2005; Nakamura & Li 2005; Martel *et al.* 2006; Tilley & Pudritz 2007).

There are several signatures of turbulence triggering. First, the cloudy structure in a turbulent medium has a power law power spectrum, which means there is no characteristic scale except the largest scale (e.g., Stützke *et al.* 1998). In fact, the morphology tends to be hierarchical, with large clouds containing small subclouds over many levels. This hierarchy in gas produces a similar hierarchy in young stars, which is evident as substructure in embedded clusters (e.g., Testi *et al.* 2000; Dahm & Simon 2005; Gutermuth *et al.* 2005), and as nested super-structures on larger scales (e.g., several subgroups are collected into each OB association, and several OB associations are collected into each star complex; see review in Elmegreen 2008a). Each galactic cluster seems to be the inner mixed region of the hierarchy, where the efficiency of star formation is automatically high (Elmegreen 2008b).

Second, the hierarchy of structures produces a mass spectrum for clusters, and nearly the same mass spectrum for stars, that is $dN/dM \propto M^{-2}$ (the Salpeter IMF would have a power -2.35). This is because each layer in the hierarchy contains the same total mass, just divided up in different ways. Because the hierarchy is a sequence in the log of the mass (each level divides up the mass of the previous higher level), we have the mass conserving requirement that $MdN/d \log M = \text{constant}$, that is, the total mass in each $\log M$ interval is constant. This converts to $M^2 dN/dM = \text{constant}$, as above. Another way to view this is to consider a hierarchy of levels where the final product of star formation, a cluster, for example, or an OB association, comes from some cloud at one of many possible levels in the hierarchy. That cloud is contained, along with other clouds, in the next higher cloud, and also is subdivided into several sub-clouds. Then it turns out that the same mass function follows by randomly sampling all clouds in the hierarchical tree. That is, if every cloud (and all of its subclouds) is equally likely to produce a stellar object as every

other cloud, then $M^2 dN/dM = \text{constant}$ again. This may be seen with a simple example. Imagine clouds subdivided by twos: one cloud of mass 32 units divided into 2 clouds of mass 16 units, which are each divided into 2 more clouds of 8 units, and so on until the smallest level, which has 32 clouds of 1 unit mass each. The total number of clouds, counting everything, is $32 + 16 + 8 + 4 + 2 + 1 = 63$. The probability that a cloud of mass 8, say, is selected, is the number of clouds with mass 8, namely 4 clouds, divided by the total number of clouds, 63. The probability that a cloud of mass 4 is chosen is similarly $8/63$. In general, the probability that a cloud of mass M is chosen is $\propto 1/M$. Since we have intervals of $\log M$ again, and we are assuming the number of clouds is proportional to their probability, we get $dN/d \log M \propto 1/M$, or $dN/dM \propto 1/M^2$, as above. Thus turbulence, and the hierarchical structure it always produces, is the likely cause of the M^{-2} mass functions for clusters and OB associations (Elmegreen & Efremov 1997), and maybe even stars.

The mass function for clouds is measured differently. Clouds are usually defined by the resolution of a survey. That is, most cloud mass functions have clouds with sizes within a factor of 10 of the survey resolution. The total span of mass is therefore only a factor of 100 (since mass is proportional to size-squared). Larger clouds are not counted because they can always be subdivided into their smaller pieces. This is a problem with defining clouds as regions inside of closed contours, for example, and of disallowing any multiple-counting of mass. Turbulent media are not really composed of separate clouds within an intercloud medium. Contours do not represent the power law structure correctly and mass spectra obtained from contours do not represent the true distribution of mass into all of its parts. For stellar structures, we can measure objects arbitrarily large (unlike the case for contoured clouds) because the stellar objects are not defined by their structure (e.g., contours) but by their stellar content: IR-excess stars, for example, define a young cluster, OB stars define an OB association, and red supergiants define a star complex (Efremov 1995). This connection between stellar types and structure nomenclature is a selection effect, resulting from the third aspect of turbulence triggering, discussed next. Also, stellar aggregates tend to be defined by friends-of-friends algorithms, which is intrinsically hierarchical, unlike contouring. Better algorithms for counting clouds have recently been devised (Rosolowsky *et al.* 2008).

Third, turbulence triggering tends to occur on the timescale for the turbulent motions to move through a region, i.e., the crossing time. Because the turbulent speed scales with a fractional power of the size, the crossing time (size divided by speed) also increases with a fractional power of the size. This means that larger regions form stars longer. This correlation has been observed in the LMC clusters and cepheids (Efremov & Elmegreen 1998). As a result, regions defined by stars with a certain age range, such as IR-excess stars, O-type stars, etc., tend to have a certain size and mass. They are not distinct objects, however. OB associations are not intrinsically different from T associations or embedded clusters or star complexes, aside from their difference in selected age range. Recall that turbulence is scale free. It is only the selection of an age that corresponds to the selection of a certain scale or mass of star formation. This is true up to the largest scale for star formation, which is a flocculent spiral arm or one of the beads-on-a-string in a stellar arm (Elmegreen & Efremov 1996; Odekon 2008).

Turbulence triggering seems to work along side sequential triggering on scales smaller than the ambient Jeans length, which is L_J defined below. This is also about the galactic scale height. Thus a simplified model for all of these processes would be that gravitational instabilities produce clouds and drive turbulence on the largest scales (L_J), while turbulence and gravitational collapse trigger the first generation of stars inside these primary clouds. Sequential triggering prolongs star formation in the debris during the process

of cloud disruption. The fractions of stars triggered by turbulence and by the various sequential processes would be interesting to observe.

4. The Cosmological Connection

Deep surveys in the optical and infrared have produced images of thousands of young galaxies, some of which are half, or even one-tenth, the age of the current universe. It is interesting to ask whether star formation in these galaxies has the same cause and morphology as local star formation.

To investigate this, we have measured regions of star formation in all of the large (> 10 pixels) galaxies in the Hubble Space Telescope Ultra Deep Field (UDF, Beckwith 2006). There are about 1000 of them (Elmegreen *et al.* 2005). Galaxies look different at high redshift. Irregular structures dominate, and interactions are relatively common (Abraham *et al.* 1996a,b; Conselice, Blackburne, & Papovich 2005). The one irregularity that seems to be most common is the presence of giant blue clumps from star formation (Elmegreen & Elmegreen 2005). These clumps are usually observed in the restframe ultraviolet because of the high redshifts involved, but even there they have absolute magnitudes that can be brighter than -18 mag (Elmegreen & Elmegreen 2006b; Elmegreen *et al.* 2007a, 2008c). Population models suggest that clump stellar masses are in the range $10^7 - 10^8 M_{\odot}$, with some clumps larger than $10^9 M_{\odot}$ (Elmegreen *et al.* 2007a, 2008c). Clump diameters are ~ 1.5 kpc, and stellar ages in the clumps are typically within a factor of 3 of 10^8 yrs (Elmegreen & Elmegreen 2005; Elmegreen *et al.* 2008c).

There are no obvious shells or comets of triggered star formation at high redshift, but none are expected at the available resolution of ~ 200 pc out to $z \sim 5$. In the most clumpy galaxies, which are the *clump clusters* and *chains* (Elmegreen *et al.* 2005), there are no spirals either, even though spiral structure would be seen at ~ 5 if it was bright enough in the uv. Other galaxies clearly have spirals and bulges. At $z > 1$, clump clusters and chains in the UDF outnumber spirals 2:1.

In a recent survey of bulge properties using H-band NICMOS observations in the UDF (Elmegreen *et al.* 2008c), we found that $\sim 50\%$ of the clump clusters and $\sim 30\%$ of the chains have bright, often central, red clumps indicative of bulges. Others may have only a red and smooth underlying disk. We also found that when there are bulges in the most clumpy galaxies, these bulges are more similar to the clumps with respect to age and mass than the bulges in spiral galaxies are to their clumps. Thus clump clusters and chains either have no bulges or they have young bulges.

Figure 1 shows a selection of UDF clump cluster galaxies without obvious bulges (from Elmegreen *et al.* 2008c, which contains a color version of this figure). Each galaxy is shown as a pair of images, with the color Skywalker image on the left and the NICMOS H-band image on the right. There are bright clumps at NICMOS-H, but nothing centralized and nothing obviously connected with a disk population; most are associated with a star formation feature, and some could be independent galaxies. Either these clump clusters will turn into late-type spirals with small bulges, or they have not yet formed their bulges. Conceivably, one of the prominent clumps could migrate to the center to make a bulge, or several could collide and make a bulge. This clump-migration model for bulge formation was proposed by Noguchi (1999) and Immeli *et al.* (2004a,b). More details and a match to observations is in recent papers by Bournaud *et al.* (2007, 2008) and Elmegreen *et al.* (2008a,c).

The recent batch of models starts with a disk that is half gas and half stars, in addition to a live halo. The stellar part is Toomre-stable but the gas+stellar disk is unstable. Almost immediately, the gas and some of the stars collapse into four or five giant clumps

with $10^8 M_{\odot}$, like the observed clumps in clump-cluster galaxies. When the disk is slightly off-center from the bulge, the clumps get flung around to large radii, as observed in UDF 6462 (Bournaud *et al.* 2008), contributing to the general appearance of irregularity. The basic process of clump formation is a gravitational instability. The collapse is rapid and it forms clumps rather than spirals because the self-gravitational forces dominate the background galactic forces. This result seems reasonable for a young galaxy primed with fresh gas from cosmological accretion. The instability has two important differences compared with that in local galaxies: first, the high gas fraction makes the clumps round rather than spiral-like, and second, a high turbulent speed makes the clumps massive. Recall that the bulk Jeans length is $L_J = 2\sigma^2/G\Sigma$ for turbulent speed σ and disk column density Σ , and the Jeans mass is $M_J = \sigma^4/G^2\Sigma$. The key to a large unstable mass is a large velocity dispersion.

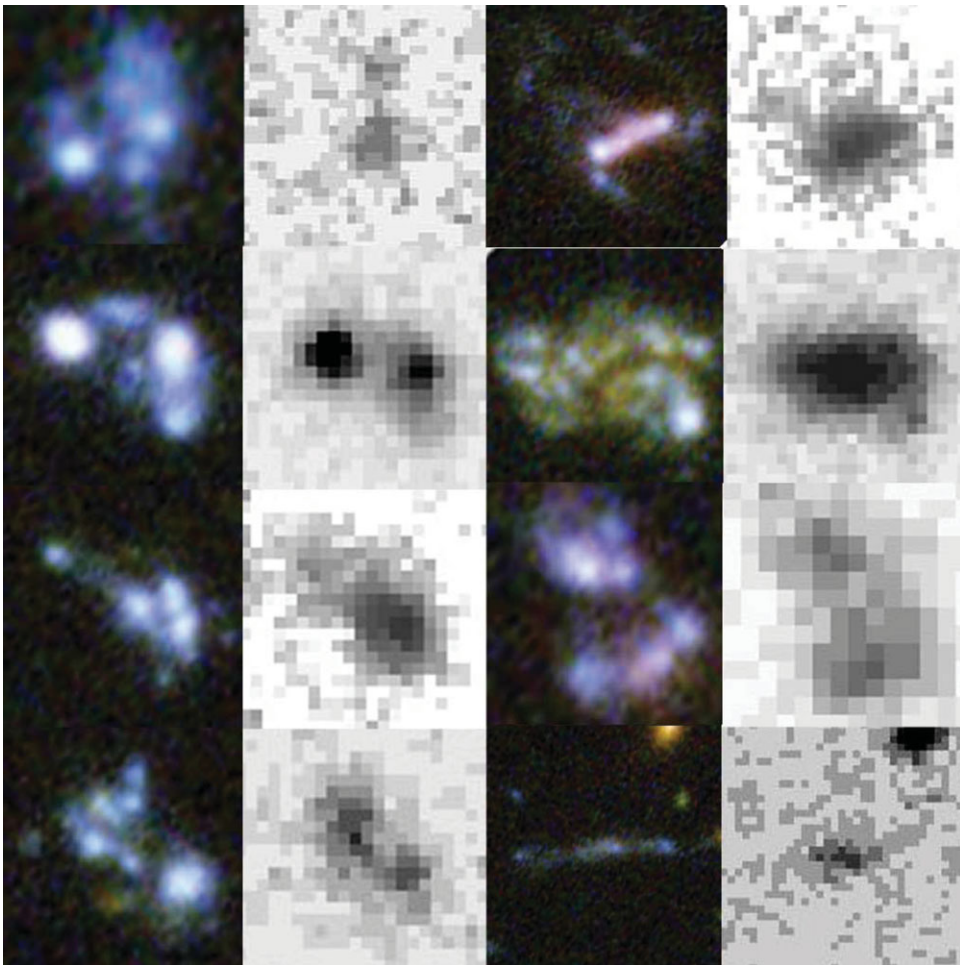


Figure 1. Eight clumpy galaxies in the UDF with no obvious central red object that might be a bulge. Each galaxy is shown twice, on the left using the high resolution of the ACS from the color Skywalker image, and on the right using the lower resolution NICMOS image in H band. Red emission is either extended in a seemingly old population of stars, or it is associated with bright star-forming regions.

The basic scales L_J and M_J come from the dispersion relation for gravitational instabilities in an infinitely thin and extended disk, which is $\omega^2 = \sigma^2 k^2 - 2\pi k G \Sigma$; $i\omega$ is the growth rate and k is the wavenumber. The wavenumber at fastest growth is obtained by setting $d\omega/dk = 0$, which gives $k_{fast} = \pi G \Sigma / \sigma^2$. The Jeans length is $L_J = 2\pi / k_{fast}$ and the Jeans mass is $M_J \sim (L_J/2)^2 \Sigma = \sigma^4 / G^2 \Sigma$, as written above. This mass could be written in a variety of ways, such as $\pi (L_J/2)^2 \Sigma$ or $(L_J)^2 \Sigma$, depending on assumptions about what constitutes a cloud; i.e., what fraction of the unstable mass gets into the cloud. The preferred form is a compromise, and selected partly to match local observations of giant cloud masses. Additional things modify the dispersion relation, such as magnetic fields, spiral arms, finite disk thickness, turbulent motions, a non-isothermal equation of state, molecule formation, and so on. Simulations reproduce many of these effects in a way that simple expressions cannot. A detailed model for star formation in a galaxy disk, such as that by Robertson & Kravtsov (2008) discussed at this conference, should do a better job of defining a characteristic scale or outer-scale for cloud formation. Still, it is useful to see how the basic observed quantities, like mass and length, vary with ISM properties.

The mass and size of star formation clumps in high redshift galaxies exceed those in local galaxies by factors of ~ 100 and ~ 3 , respectively. Thus σ^2 has to increase by $100/3 \sim 30$, which means that σ has to increase by $\times 5.5$, making it 30 or 40 km s⁻¹ instead of the local 6 or 7 km s⁻¹. This requirement is satisfied by the observation of high velocity dispersions in high redshift galaxies (Förster Schreiber, *et al.* 2006; Genzel *et al.* 2006, 2008; Weiner *et al.* 2006). Similarly, Σ has to be larger by a factor of $100/3^2 \sim 10$ at high redshift. The gaseous disks of local spiral galaxies have $\Sigma \sim 10 M_\odot \text{ pc}^{-2}$, which makes $M_J \sim 2 \times 10^7 M_\odot$, comparable to the observed local gas clump mass, for $\sigma = 6 \text{ km s}^{-1}$. At high redshift, the unstable column density in the disk has to be $\sim 100 M_\odot \text{ pc}^{-2}$, which is comparable to the total mass column density of the inner regions of today's spirals. Considering that high redshift spiral galaxies are slightly smaller than today's spirals (Elmegreen *et al.* 2007b), the clump clusters and chains could be forming the inner thick disks and bulges of today's galaxies.

A big uncertainty for star formation studies of high redshift galaxies is the neutral gas abundance. CO has been observed in several galaxies (Solomon & Vanden Bout 2005; Tacconi *et al.* 2008) but with little resolution into clouds. HI has not been observed in emission yet and the absorption of HI, in the form of damped Lyman α lines, has an unknown geometry relative to stellar galaxies (Wolfe *et al.* 2008). CO is also present in DLA gas (Srianand *et al.* 2008). Quite possibly, the gas mass is comparable to or larger than the observed stellar mass, and the gas is as irregular as the stars in these clumpy disks. Our prediction is that the velocity dispersion of the neutral gas should be high, something like 40 km s⁻¹ or more, which is observed for the ionized gas. The dispersion inside the clumps should be high also, although perhaps not quite as high if only the cores are observed in molecular transitions.

There are two other pieces of evidence that star formation is prompted by gravitational instabilities in high redshift disks. First there is a linear alignment of clumps in chain galaxies, which are presumably edge-on clumpy disks. Clump positions are aligned along the midplane of the chain to within a fraction of a pixel (Elmegreen & Elmegreen 2006a) or $\sim 100 \text{ pc}$, on average (i.e., for 112 chain galaxies in the UDF). This implies that most clumps are not extragalactic objects in the process of coalescence; they formed in a pre-existing disk. Second, a large fraction of interacting galaxies with tidal features and rings have regularly spaced clumps in those features (Elmegreen *et al.* 2007a). They therefore had to form there, and their separation should be comparable to L_J . This gives the same requirement on velocity dispersion as the clumps in non-interacting disks.

5. Conclusions

Giant cloud formation is often triggered by gravitational and associated instabilities in gas disks. The clump scale is ~ 600 pc for local galaxies, and what forms is a “star-complex,” composed of OB associations and dense clusters with $10^5 - 10^6 M_{\odot}$ of stars. The cloud mass at the beginning of the process is $\sim 10^7 M_{\odot}$. Most of this gas is in the form of low-density HI except in the dense inner regions of galaxies, where it can be largely molecular because of the higher ambient pressure.

In high-redshift disks, the clump scale is larger, ~ 1500 pc, and the stellar mass is larger, $\sim 10^7 - 10^8 M_{\odot}$. The associated gas mass in a clump is unknown but may be $10^8 - 10^9 M_{\odot}$ with much of that molecular. This scale-up of star formation at high z seems to be the result of a high turbulent speed, which, combined with a higher gas column density, makes the gravitational length and characteristic mass larger by factors of ~ 3 and ~ 100 , respectively.

In local galaxies, star formation begins quickly in cloud cores once they become self-gravitating. There is no reason to think otherwise for high redshifts. Locally, the cloud cores are cold, dense, molecular, magnetic, and turbulent – all necessary attributes contributing to star formation in one way or another (including the requirement of angular momentum loss during star formation). The same should be true at high redshift too. Outside the local dense cores, star formation lingers in isolated cloud debris and it can be triggered for a long time in the dispersing cloud envelopes. The analogous final stages of star formation at high redshift are unknown. Cloud dispersal by star formation feedback should be more difficult with a higher velocity dispersion (Elmegreen *et al.* 2008b). If this difficulty increases the efficiency of star formation, then comparatively little gas could remain in the cloud envelopes for prolonged triggering. Generally, cloud envelopes are more stable than their cores because of the envelope exposure to background starlight and the resulting longer magnetic diffusion time. This is why triggering can be important in the final stages of cloud disruption: compression enhances the diffusion rate while it shortens the dynamical time, causing low density regions to form stars where they otherwise would not. There is no evidence for sequentially-triggered star formation at high redshift, however, but the resolution is not good enough yet to see it.

Other differences between low and high redshift star formation concern the fate of the stellar clumps. At low z , where the disk gas fraction is low and the clump formation and evolution times are comparable to the shear time, star-forming clumps dissolve slowly into star streams and add to the thin disk without changing their galactocentric radii. At high z , clump formation appears to be much more violent and rapid compared to background galactic processes. This is observed directly in clump clusters and chain galaxies, and it is true to a certain degree also in spirals, where the clumps are more massive than they are locally. These differences follow from the observed relatively high turbulent speed and the expected high gas mass fraction. Simulations suggest that the clumps in the most clumpy disks interact with each other, stir the preexisting stars to make a thicker disk, shed half of their own stars during these interactions to add to this thick disk, and then spiral in the remaining half to make or add to a bulge.

The general theme of this conference is to understand the formation and structure of the Milky Way in the context of various models and observations of galaxies on cosmological scales. In terms of star formation, the youngest resolvable disk galaxies look both strange, in terms of their increased clumpiness, and familiar, in terms of the likely processes involved. Simulations can reproduce the basic structures without difficulty if they start with ideal initial conditions. At some point, however, the galaxy formation process has to be important, and this involves the gas accretion rate and geometry, and the galaxy interaction rate. It is more difficult to understand these aspects of young galaxies without the local analogues that are so revealing for star formation.

References

- Abraham, R., Tanvir, N., Santiago, B., Ellis, R., Glazebrook, K., & van den Bergh, S. 1996a, *MNRAS*, 279, L47
- Abraham, R., van den Bergh, S., Glazebrook, K., Ellis, R., Santiago, B., Surma, P., & Griffiths, R. 1996b, *ApJS*, 107, 1
- Bate, M. R. & Bonnell, I. A. 2005, *MNRAS*, 356, 1201
- Beckwith, S. V. W., *et al.* 2006, *AJ*, 132, 1729
- Bonnell, I. A., Dobbs, C. L., Robitaille, T. P., & Pringle, J. E. 2006, *MNRAS*, 365, 37
- Bonnell, I. A., Larson, R. B., & Zinnecker, H. 2007, in: B. Reipurth, D. Jewitt, & K. Keil (eds), *Protostars and Planets VI* (Tucson, Univ of Arizona), p. 149
- Bournaud, F., Elmegreen, B. G., & Elmegreen, D. M. 2007a, *ApJ*, 670, 237
- Bournaud, F., Daddi, E., Elmegreen, B. G., Elmegreen, D. M., & Elbaz, D. 2008, *A&A* in press, [astro-ph/0803.3831](https://arxiv.org/abs/astro-ph/0803.3831)
- Brinks, E. & Bajaja, E. 1986, *A&A*, 169, 14
- Conselice, C. J., Blackburne, J. A., & Papovich, C. 2005a, *ApJ*, 620, 564
- Dahm, S. E. & Simon, T. 2005, *AJ*, 129, 829
- de Geus, E. J. 1992, *A&A*, 262, 258
- Dekel, A. & Silk, J. 1986, *ApJ*, 303, 39
- Dobbs, C. L. & Bonnell, I. A. 2007, *MNRAS*, 374, 1115
- Efremov, Y. N. 1995, *AJ*, 110, 2757
- Efremov, Yu. N. & Elmegreen, B. G. 1998, *MNRAS*, 299, 588
- Elmegreen, B. G. 1994, *ApJ*, 427, 384
- Elmegreen, B. G. 2007, *ApJ*, 668, 1064
- Elmegreen, B. G. 2008a, in: A. de Koter, L. J. Smith, & L. B. F. M. Waters (eds), *Mass Loss from Stars and the Evolution of Stellar Clusters* (San Francisco: Astronomical Society of the Pacific), p. 249
- Elmegreen, B. G. 2008b, *ApJ*, 672, 1006
- Elmegreen, B. G. & Efremov, Y. N. 1996, *ApJ*, 466, 802
- Elmegreen, B. G. & Efremov, Y. N. 1997, *ApJ*, 480, 235
- Elmegreen, B. G., Palous, J., & Ehlerova, S. 2002, *MNRAS*, 334, 693
- Elmegreen, B. G. & Elmegreen, D. M. 2005, *ApJ*, 627, 632
- Elmegreen, D. M., Elmegreen, B. G., Rubin, D. S., & Schaffer, M. A. 2005, *ApJ*, 631, 85
- Elmegreen, B. G. & Elmegreen, D. M. 2006a, *ApJ*, 650, 644 thick disks
- Elmegreen, D. M. & Elmegreen, B. G. 2006b, *ApJ*, 651, 676 rings bend chains
- Elmegreen, D. M., Elmegreen, B. G., Ferguson, T., & Mullan, B. 2007a, *ApJ*, 663, 734 tidal tails
- Elmegreen, D. M., Elmegreen, B. G., Ravindranath, S., & Coe, D. A. 2007b, *ApJ*, 658, 763
- Elmegreen, B. G., Bournaud, F., & Elmegreen, D. M. 2008a, *ApJ*, 684, in press
- Elmegreen, B. G., Bournaud, F., & Elmegreen, D. M. 2008b, *ApJ*, submitted
- Elmegreen, D. M., Elmegreen, B. G., Fernandez, M. X., & Lemonias, J. J. 2008c, *ApJ*, submitted
- Engargiola, G., Plambeck, R. L., Rosolowsky, E., & Blitz, L. 2003, *ApJS*, 149, 343
- Förster Schreiber, N. M., *et al.* 2006, *ApJ*, 645, 1062
- Fuchs, B., Dettbarn, C., & Tsuchiya, T. 2005, *A&A*, 444, 1
- Garcia-Burillo, S., Guelin, M., & Cernicharo, J. 1993, *A&A*, 274, 123
- Genzel, R., *et al.* 2006, *Nature*, 442, 786
- Genzel, R., *et al.* 2008, *ApJ*, in press, [aarXiv:0807.1184](https://arxiv.org/abs/aarXiv:0807.1184)
- Gutermuth, R. A., Megeath, S. T., Pipher, J. L., Williams, J. P., Allen, L. E., Myers, P. C., & Raines, S. N. 2005, *ApJ*, 632, 397
- Hester, J. *et al.* 1996, *AJ*, 111, 2349
- Immeli, A., Samland, M., Gerhard, O., & Westera, P. 2004a, *A&A*, 413, 547
- Immeli, A., Samland, M., Westera, P., & Gerhard, O. 2004b, *ApJ*, 611, 20
- Jappsen, A.-K., Klessen, R. S., Larson, R. B., Li, Y., & Mac Low, M.-M. 2005, *A&A*, 435, 611
- Kim, Chang-Goo; Kim, Woong-Tae; Ostriker, & Eve C. 2006, *ApJ*, 649, L13
- Kim, W.-T. & Ostriker, E. C. 2002, *ApJ*, 570, 132
- Kim, W.-T., Ostriker, E. C., & Stone, J. M. 2003, *ApJ*, 599, 1157

- Kosiński, R. & Hanasz, M. 2006, *MNRAS*, 368, 759
- La Vigne, M. A., Vogel, S. N., & Ostriker, E. C. 2006, *ApJ*, 650, 818
- Lee, S. M. & Hong, S. S. 2007, *ApJS*, 169, 269
- Li, P. S., Norman, M. L., Mac Low, M.-M., & Heitsch, F. 2004, *ApJ*, 605, 800
- Luna, A., Bronfman, L., Carrasco, L., & May, J. 2006, *ApJ*, 641, 938
- Lundgren, A. A., Olofsson, H., Wiklund, T., & Rydbeck, G. 2004, *A&A*, 422, 865
- Mac Low, M.-M. & Klessen, R. S. 2004, *RvMP*, 76, 125
- Martel, H., Evans, N. J., II, & Shapiro, P. R. 2006, *ApJS*, 163, 122
- Nakamura, F. & Li, Z.-Y. 2005, *ApJ*, 631, 411
- Noguchi, M. 1999, *ApJ*, 514, 77
- Odekon, M. C. 2008, *ApJ*, 681, 1248
- Oey, M. S., Watson, A. M., Kern, K., & Walth, G. L. 2005, *AJ*, 129, 393
- Padoan, P., Kritsuk, A., Norman, M. L., & Nordlund, A. 2005, *Memorie della Societa Astronomica Italiana*, 76, 187
- Reach, W. T., *et al.* 2004, *ApJS*, 154, 385
- Robertson, B. E. & Kravtsov, A. V. 2008, *ApJ*, 680, 1083
- Rosolowsky, E. W., Pineda, J. E., Kauffmann, J., & Goodman, A. A. 2008, *ApJ*, 679, 1138
- Solomon, P. & Vanden Bout, P. 2005, *ARA&A*, 43, 677
- Srianand, R., Noterdaeme, P., Ledoux, C., & Petitjean, P. 2008, *A&A*, 482, L39
- Stützi, J., Bensch, F., Heithausen, A., Ossenkopf, V., & Zielinsky, M. 1998, *A&A*, 336, 697
- Sugitani, K., Fukui, Y., Mizuni, A., & Ohashi, N. 1989, *ApJ*, 342, L87
- Tacconi, L. J. *et al.* 2008, *ApJ*, 680, 246
- Testi, L., Sargent, A. I., Olmi, L., & Onello, J. S. 2000, *ApJ*, 540, L53
- Tilley, D. A. & Pudritz, R. E. 2007, *MNRAS*, 382, 73
- Tosaki, T., Hasegawa, T., Shioya, Y., Kuno, N., & Matsushita, S. 2002, *PASJ*, 54, 209
- Yamaguchi, R., Mizuno, N., Onishi, T., Mizuno, A., & Fukui, Y. 2001a, *PASJ*, 53, 959
- Yamaguchi, R., Mizuno, N., Onishi, T., Mizuno, A., & Fukui, Y. 2001b, *PASJ*, 553, L185
- Walter, F. & Brinks, E. 1999, *AJ*, 118, 273
- Weiner, B. J., *et al.* 2006, *ApJ*, 653, 1027
- Whitworth, A. P., Bhattal, A. S., Chapman, S. J., Disney, M. J., & Turner, J. A. 1994, *A&A*, 290, 421
- Wilcots, E. M. & Miller, B. W. 1998, *AJ*, 116, 2363
- Wolfe, A. M., Prochaska, J. X., Jorgenson, R. A., & Rafelski, M. 2008, arXiv:0802.3914
- Zavagno, A., Deharveng, L., Comerón, F., Brand, J., Massi, F., Caplan, J., & Russeil, D. 2006, *A&A*, 446, 171



Coffee break. Camilla Juul Hansen and Anna Árnadóttir outside the lecture hall.



From the Saturday excursion to Hven. The group tries, with mixed success, to emulate the posture of the statue of Tycho Brahe. Photo: Bruce Elmegreen (in front, at centre).